

Performance of wave breaker formulations in SWAN

CTB3000-16: Bachelor eindwerk
Matthijs (M.I.O.) Wanrooij

Performance of wave breaker formulations in SWAN

by

Matthijs (M.I.O.) Wanrooij

Student Name	Student Number
Matthijs Wanrooij	5142040

Instructor: Dr. ir. M. (Marcel) Zijlema
Second reader: Dr. T.S. (Ton) van den Bremer
Project Duration: February 13, 2023 - April 3, 2023
Faculty: Faculty of Civil Engineering and Geosciences, Delft

Cover: Zeeland, Netherlands by ESA under CC BY-SA 3.0 IGO (Modified)
Style: TU Delft Report Style, with modifications by Daan Zwanenveld



Preface

This introductory level research project serves as the final milestone for completing the bachelor degree of Civil Engineering at Delft University of Technology. In the first place, I would like to thank my supervisor Dr. ir. M. Zijlema for his patient support and the many useful suggestions. My gratitude also extends to Dr. T.S. van den Bremer for being my second reader and to J.A. Garcia for being present at my midterm presentation. It has been a pleasure to work on this project which has been as much a culminating effort representing the preceding three years as it has been a source of new insights.

*Matthijs (M.I.O.) Wanrooij
Delft, April 2023*

Summary

Depth-induced wave breaking is a complex process that is approached mainly through heavily parameterized models. Recent refinements in wave breaker formulations are manifold but exclude a frequency dependence in the dissipation. This research project aims to examine whether such an omission is justified. To this end, observational results from the Hinderplaat shoal in the Haringvliet estuary (Netherlands) are compared with simulated wave spectra through a dissipation coefficient that is evaluated at two trajectories over the shoal. Simulations are carried out in SWAN. Dissipation coefficients are subjected to a z-test based on Kendall's tau coefficient to detect statistically significant trends in the frequency dependence. Significant frequency dependence is established for one trajectory at a significance level of 0.05. It is however found that the observational spectrum underlying the dissipation coefficient for this trajectory shows divergent characteristics that make its application to the problem unreliable. Based on these results, no conclusion is reached on the presence of a frequency dependence in the dissipation. Instead, a series of recommendations is put forth to improve results with relatively slight adjustments to the methodology.

Contents

Preface	i
Summary	ii
Nomenclature	iv
1 Introduction	1
1.1 Problem statement	1
1.2 Relevance	2
1.3 Advances in literature	2
1.4 Outline of approach	3
2 Analysis Procedure in SWAN	6
2.1 Processing pipeline	6
2.2 Model comparison	6
2.3 Model configurations	7
3 Discussion of results	9
3.1 General remarks	9
3.2 Assessment of interpolation effects	9
3.3 Dissipation coefficients	10
3.4 Comparison of dissipation coefficients with Chen et al. (1997), Kuznetsov and Saprykina (2004) and Meza et al. (2002)	12
4 Conclusion and outlook	14
Bibliography	15
A Source Code	17
B Some background on statistical testing with Kendall's tau coefficient for α_1 and α_2	18
C Simulated results: frequency-direction spectral plots	20
D Interim evaluation: roadmap and peer review	23

Nomenclature

Abbreviations

Abbreviation	Definition
CONSTANT	Battjes and Janssen (1978) constant breaker index formulation
BKD	J. Salmon et al. (2015) bottom slope and dimensionless depth scaling breaker index formulation
DCTA	Booij et al. (2009) Distributed Colinear Triad approximation
DEWIT	de Wit (2022) parametrization of the biphase evolution based on local bed slope and peak wave period
ELDEBERKY	Eldeberky (1996) biphase parametrization as a function of Ursell number
LTA	Eldeberky (1996) Lumped Triad Approximation
SPB	Becq-Girard et al. (1999) Stochastic Parametric model based on Boussinesq equations
WESTHUYSEN	Van der Westhuysen (2009) formulation

1

Introduction

1.1. Problem statement

When waves approach the shore, the ratio between wave amplitude and water depth increases, causing instability and eventually collapse of the wave. This process is called depth-induced wave breaking or ‘surf breaking’, since the region that features breaking – in the vicinity of the shore – is referred to as the ‘surf zone’. During breaking, part of the energy contained in the wave is dissipated, mainly due to a conversion into turbulent kinetic energy near the free surface (Rapp & Melville, 1990). Additionally, conservation of momentum creates a force perpendicular to the shore (driving wave set-up) and one in the parallel direction (driving longshore drift). The specifications of the wave breaking process depend on many environmental factors such as bottom topography and wind details which, combined together, give it a rich but also highly complex and nonlinear nature. Roughly speaking, four basic types of breaking waves are recognized: the spilling, plunging, collapsing and surging type. These are illustrated in Figure 1.1.

As a consequence of the complexity of the wave breaking process, wave breaker formulations often rely heavily on parameterized models (J. Salmon & Holthuijsen, 2015). Various formulations, such as the formulation by Battjes and Janssen (1978), deal with dissipation due to depth-induced breaking for spectral wave models. Battjes and Janssen originally used a fixed, constant calibration parameter $\gamma_{BJ} = 0.8$ to relate maximum possible individual wave height to local depth. Nowadays, the value $\gamma_{BJ} = 0.73$ is used as it is averaged over a more extensive data set (Battjes & Stive, 1985). Nevertheless, the approach of using a fixed calibration parameter has demonstrated considerable effectiveness – in particular over sloping beach profiles – and consequently it features in many third-generation spectral wave models even though these rely to a great extent on improved formulations to model wave processes (J. Salmon & Holthuijsen, 2015). Off late, Westhuyzen (2010) has reported scaling issues for the calibration parameter γ_{BJ} , showing in particular that $\gamma_{BJ} = 0.73$ overestimates the dissipation of locally generated waves in horizontal bathymetries. Recent parametrizations by Van der Westhuyzen (2009) and Westhuyzen (2010) and by J. Salmon et al. (2015), which is referred to as the BKD-parametrization, use variable scalings for γ_{BJ} . Both alternatives perform better in predicting significant wave height of locally generated waves over 1D horizontal bathymetries (J. Salmon & Holthuijsen, 2015), with Salmon and Holthuijsen

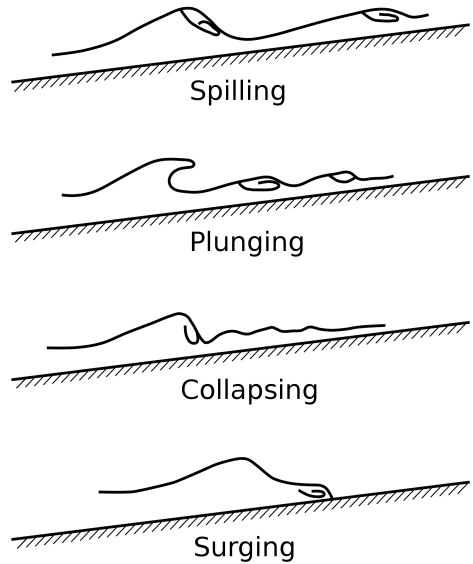


Figure 1.1: Schematic drawing of a spilling, plunging, collapsing and surging wave (Wikimedia Commons, 2015).

reporting up to 50% error reduction for both locally and non-locally generated waves. In the study, a joint scaling method for γ_{BJ} depending on both local bottom slope and normalized wave number was used and model performance was assessed by comparing results with a broad range of observational data sets (J. Salmon et al., 2015). Even though the wave breaker formulations mentioned above have become increasingly complex and refined, none of them feature a frequency dependence. The aim of this project is to verify whether this assumption is justified and, if possible, to propose a suitable adjustment to the surf breaker formulations in order to include frequency dependence.

1.2. Relevance

From an engineering perspective, information about the frequency of waves in the surf zone is relevant mainly from a sediment transport viewpoint. Puleo et al. (2000) found that low-frequency wave components are especially influential in governing sediment transport in the swash-zone (the landward edge of the surf zone). Morphodynamically, Wright and Short (1984) report differences in the deposition of sediment on beaches that are characterised by different values of a surf-scaling parameter, which in turn depends on incident wave frequency. In particular, a fully dissipative and a highly reflective limit were derived which morphologically correspond to flat, shallow beaches with large underwater sand storage and to steep beaches with small underwater sand storage. The ability to quantitatively estimate the frequency dependence of dissipation in the surf zone will improve understanding of sediment transport in this region.

1.3. Advances in literature

A thorough search in literature has revealed that the inclusion of frequency dependent terms in wave breaker formulations is a relatively unexplored topic. However, some advances are worth mentioning. Based on lab tests with unidirectional transient wave trains, Meza et al. (2000) report that energy loss due to breaking is present almost exclusively at frequencies higher than the peak frequency. They also find that wave components near the peak frequency are hardly affected by wave breaking (even though most of the energy is concentrated in this region of the spectrum) and that frequencies significantly below the peak frequency gain part of the energy lost by higher frequency waves (about 12%).¹ Based on these conclusions, Meza et al. (2002) propose that the dependence of dissipation rate S_{dis} on frequency follows the relation:

$$S_{dis} = \left(\frac{\omega}{\omega_p} \right) \left(1 - \left(\frac{\omega}{\omega_p} \right) \right) E(\omega) \quad (1.1)$$

where ω_p represents the frequency of the spectral peak.

Based on 10 test cases, Chen et al. (1997) found that the observed evolution of the wave spectrum across the surf zone is more accurately modeled when dissipation is increased at high frequencies. However, no decision on the exact formulation of the frequency dependent dissipation was reached since the predicted spectra were qualitatively correct for a broad range of frequency dependent dissipations. It was reasoned that the reduction of energy at high frequencies is counteracted to large extent by an influx of energy originating from increased nonlinear energy transfer. In the study, frequency-independent and frequency-dependent Boussinesq models were compared, where the dependence was weighted towards high frequency with an f^2 and f^4 scaling.

Research by Kuznetsov and Saprykina (2004) suggests that a distinction is made in the mechanism of wave energy dissipation relating to the inner and the outer surf zone. For the outer surf zone, it was found that dissipation is almost independent of frequency and is approximated accurately by a constant model. In contrast, the dissipation in the inner surf zone is more accurately described by a quadratic or selective frequency dependence, depending on the degree of wave asymmetry and bed slope.

¹This observation agrees with the notion of Melville (1996) that breaking might be a source of energy for waves in the low-frequency band. However, he did not succeed in constructing a quantitative relation for this purpose. An earlier model by Longuet-Higgins (1969) (which was aptly coined the 'maser' model after the device that amplifies electromagnetic waves) did attempt to devise a treatment in which the breaking of short waves could provide energy to long waves, but it was discredited by Hasselmann (1971).

The apparent contradiction between results by Chen et al. (1997) and Kuznetsov and Saprykina (2004) may derive from several differences in the model setup. In the first place, Chen et al. (1997) model the evolution of the wave spectra near and across the surf zone with the modified Boussinesq equations for normally incident nondissipative waves propagating over parallel depth contours, according to work by Chen and Liu (1995). It is then extended into the surf zone by including a breaking-induced dissipative term based on a dissipation function that is chosen to match another model (specifically, the frequency-integrated energy balance model of Whitford (1988)). On the other hand, Kuznetsov and Saprykina (2004) use Boussinesq-type equations with improved dispersion characteristics that have been shown to match experimental results for describing the transformation of waves over an inclined bed at certain relative water depths. Secondly, the initial conditions and the beach profiles under consideration differ. In Chen et al. (1997), experimental results are taken from two datasets in the Black Sea and North Sea, both in the month of October. Meanwhile, Kuznetsov and Saprykina (2004) use a more diverse dataset.

1.4. Outline of approach

To investigate the frequency dependence of surf breaking, simulated results are compared with observational data. The simulations for this project are carried out in SWAN 41.41 for Windows. SWAN (*Simulating WAves Nearshore*) is a third-generation wave model that computes random, short-crested wind-generated waves in coastal regions and inland waters. SWAN is developed and supported by Delft University of Technology (TU Delft, Netherlands) and has many scientific and practical applications (Fluidmechanics Section, Delft University of Technology, n.d.).

From a technical perspective, SWAN works by solving the action balance equation:

$$\frac{\partial}{\partial t}N + \frac{\partial}{\partial x}c_xN + \frac{\partial}{\partial y}c_yN + \frac{\partial}{\partial \sigma}c_\sigma N + \frac{\partial}{\partial \theta}c_\theta N = \frac{S}{\sigma} \quad (1.2)$$

Here N , the action density, depends on intrinsic frequency σ , direction θ , spatial coordinates x and y (coinciding with the ocean plane) and time t : $N(\sigma, \theta, x, y, t)$. The c -terms represent propagation velocities of the underscored variables in their respective spaces (i.e. $c_x = \partial x / \partial t$), while the S -term on the right hand side represents a source term accounting for generation, dissipation and nonlinear wave-wave interaction. The fourth and fifth term describe, in that order, the contribution due to shifting of the relative frequency (due to changes in depth and current) and the depth- and current-induced refraction. We thus see that the action balance equation encompasses the effects of spatial propagation, refraction, shoaling, generation, dissipation and nonlinear wave-wave interactions (Ris et al., 1999). The full technical details for the SWAN-model are provided in Fluidmechanics Section, Delft University of Technology (2023a).

The area of study for this project concerns the Hinderplaat, a flat shoal in front of the Haringvliet. The Haringvliet is a dammed tidal delta with an area of roughly 10×10 [km], located in the southwestern part of the Netherlands. The Hinderplaat shoal partly shields the inlet of the Haringvliet from the Southern North Sea. Average water depth in the area varies between 4 and 6 [m], while over the Hinderplaat depth varies between 1.0 and 2.2 [m]. The slope of the shoal measured in the direction of mean wave propagation varies from horizontal to 1:500 at the crest (J. Salmon & Holthuijsen, 2015).

Due to the relative decrease of water depth over the shoal, waves approaching the Haringvliet delta are subjected to surf breaking and hence, their energy is partly dissipated over the shoal. Observational data for 8 locations before and after the Hinderplaat is available. This data was gathered during a storm in the Haringvliet in 1982. The particular dataset has been selected because of the presence of a fairly constant wind, high waves and a water level that is low enough to allow generation of a secondary spectral peak in the proximity of the shoal, while still covering the shoal with water (Xi advies bv, n.d.). The locations of the measurement stations are indicated in Figure 1.2.

Quantification of surf breaking induced dissipation as a function of frequency over the Hinderplaat shoal is handled through the dissipation coefficient α_n , as stated in Saprykina et al. (2022):

$$\alpha_n = \frac{S(x_{start} + \Delta x)_{calc} - S(x_{start} + \Delta x)_{meas}}{S(x_{start})_{meas}(2\Delta x)} \quad (1.3)$$

In this formula, S represents the wave spectrum taken at two points separated by a distance Δx , while the indices ‘meas’ and ‘calc’ identify whether spectral data is provided through observation or through simulation, respectively. If $S(x_{start} + \Delta x)_{calc}$ is taken as the simulated wave spectrum *without* the contribution of surf breaking, subtracting the measured spectrum (which naturally includes all source terms) from the simulated spectrum in the numerator of α_n isolates the contribution of breaker terms. If the resulting α_n has a strong frequency dependence, it is evident that the process of surf breaking is not accurately modelled by a frequency independent formulation.

Generation of wave spectra in SWAN depends in part on the simulation of nonlinear wave-wave interactions. Nonlinear wave-wave interactions cause resonant sets of wave components to exchange energy such that the energy is redistributed over the spectrum. In deep and intermediate water, this process occurs predominantly through four-wave interactions (*quadruplets*), whereas in shallow water, three-wave interactions (*triads*) take on a major role. Triad wave-wave interactions have been shown to transfer energy from lower to higher frequencies, contributing to higher harmonics. Energy transfer in triad interactions can take place over relatively short distances and has been observed to change single-peaked spectra into multi-peaked spectra (Beji & Battjes, 1993; Fluidmechanics Section, Delft University of Technology, 2023a).

In this project, the DCTA (Distributed Colinear Triad approximation) parametrization for the nonlinear triad interaction is used . Specifically, the biphase formulation as a function of Ursell number by Eldeberky (Eldeberky, 1996) is employed. All technical formulations and parametrizations will henceforth be referred to in accordance with the names specified in the Nomenclature.

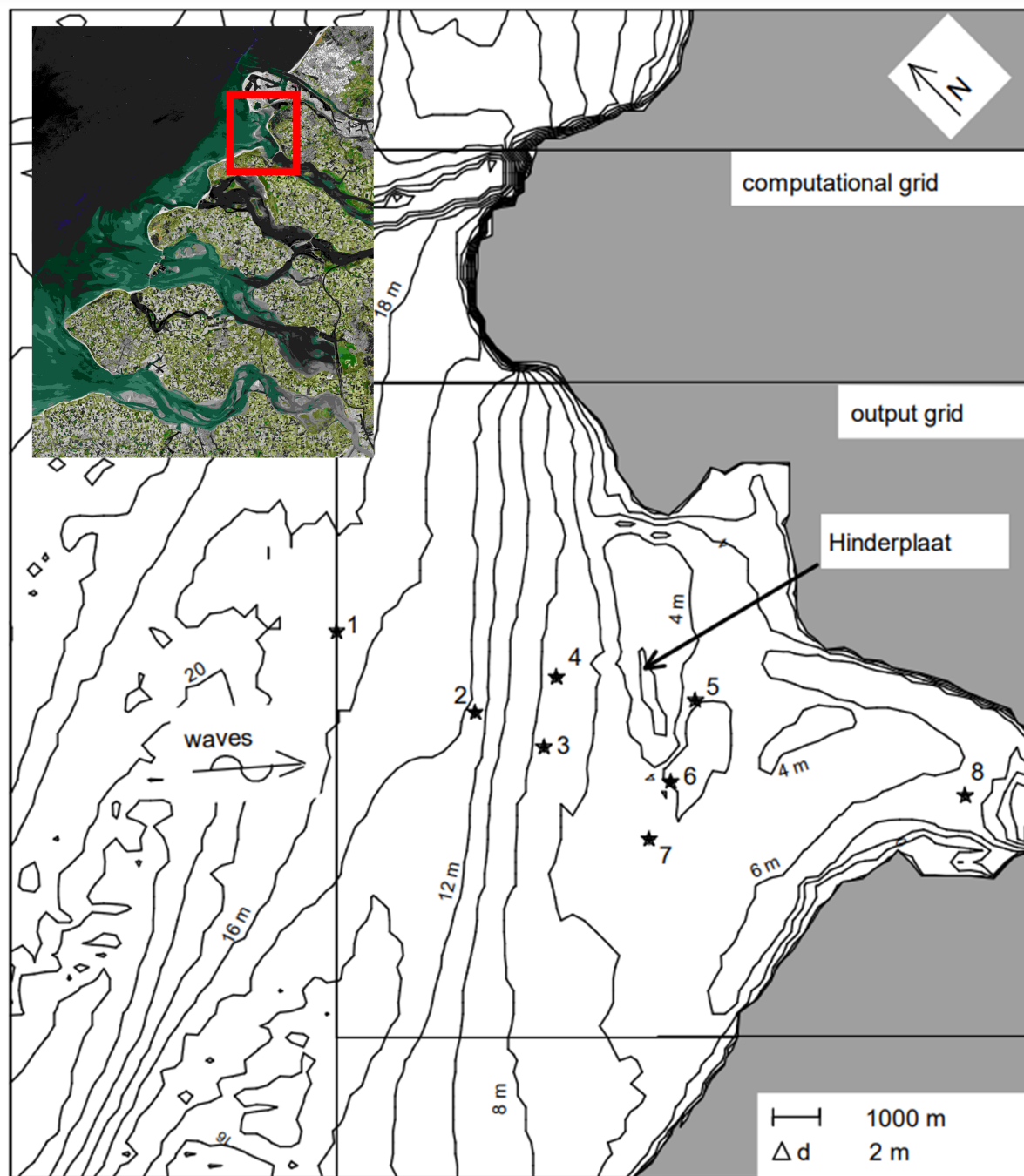


Figure 1.2: Bathymetry of the Haringvliet estuary, showing the Hinderplaat shoal and various isolines indicating average water depth. The inset shows the situation of the Haringvliet in relation to the topography of Zeeland (Southern Netherlands). The locations of eight observation stations are marked by stars. Main image taken from Xi advies bv (n.d.). Inset adapted from European Space Agency (2020).

2

Analysis Procedure in SWAN

In this chapter, the analysis procedure for the simulations is outlined. First, a processing pipeline is presented to describe the flow of simulation and to lay a foundation for analysis of the results. Then, the model configurations and the choice of parameter space are discussed.

2.1. Processing pipeline

Figure 2.1 gives an overview of the pipeline that is used to simulate and process the data for this project. Interaction with SWAN occurs through a terminal user interface. A simulation is set up in a SWAN-command file (.swn file) that contains a set of commands specifying model description and output, supplemented by start-up and lock-up commands that are of no interest to this chapter. To facilitate identification, SWAN-commands will be written in verbatim (VERBATIM) mode. Fluidmechanics Section, Delft University of Technology (2023b) contains detailed documentation of SWAN-commands and command file structure, while Fluidmechanics Section, Delft University of Technology (2023a) contains technical details and background on the SWAN-program.

The model description can be decomposed into commands for the computational grid, input fields, boundary and initial conditions, model physics and model numerics. Some specifications concerning input fields, boundary conditions and desired output locations on the grid are supplied to the command file by way of references to external files, which are subsequently recognized and read in by the interpreter in the execution phase. Input fields cover such aspects as dimensions of bottom, water level, current and friction grid, as well as wind. Model physics covers the desired generation for the program to run in (GEN1, GEN2, GEN3) and specifications for physical processes such as dissipation by white-capping, quadruplet wave-wave interactions, depth-induced wave breaking, bottom friction and triad wave-wave interactions.

Output of modelled quantities is possible in multiple formats. For the project at hand, spectral output (supplied via the SPECOUT command) is relevant. The main results will be derived from one-dimensional spectral data (specified with SPEC1D). Two-dimensional spectral data (SPEC2D) is only used in a visual way to verify trends and as a tool for intuition. For processing two-dimensional spectral SPEC2D-data in Python, the package *Wavespectra* v. 3.13.0 is used (Durant et al., 2023). SPEC1D-data is processed using a spectrum analyzer that was custom-made for this project. The full spectrum analyzer is available from the author upon request.

It is remarked that the spectrum analyzer has been configured to handle missing values in the SWAN-output (indicated by a -0.9900E+01, -0.9900E+02 or -0.9900E+03 value) through substitution with a NaN-placeholder.

2.2. Model comparison

To estimate the effect of the Hinderplaat shoal on surf breaking, we study the dissipation coefficient. The dissipation coefficient is calculated over two linear trajectories along the shoal, specified by the

locations 3 and 4 for the first point (before the shoal) and 5 and 6 for the second point (after the shoal; see Figure 1.2). J. E. Salmon (2016, p. 74) argued that the wavefield at the Hinderplaat is dominated by non-local waves that originate a large distance away from the shore. Because SWAN generates contributions locally (over the input grid), it is justified to disable all deep water processes in SWAN when simulating the wavefield in location 5 and 6. These include contributions from windgrowth, nonlinear quadruple wave interactions, whitecapping and surf breaking (they can be turned off with the OFF command in the SWAN-command file). What remains are contributions from shallow water physics, namely nonlinear triad interactions and bottom friction. As indicated in the introduction the, nonlinear triad source parametrization that will be used is DCTA BIPHASE ELDEBERKY.

Calculated spectra are compared through the dissipation coefficient with measured spectra in the points 5 and 6, which naturally include all contributions to the wavefield, including those of surf breaking, bottom friction and nonlinear triad interactions. Following this approach, we can formulate:

$$\alpha_1 = \frac{S_{calc,5}^{nl3,fr} - S_{meas,5}}{2\Delta x S_{meas,4}} \quad (2.1)$$

$$\alpha_2 = \frac{S_{calc,6}^{nl3,fr} - S_{meas,6}}{2\Delta x S_{meas,3}} \quad (2.2)$$

Here, Δx , the distance between point 4 and 5 and between point 3 and 6, is put at 2000 [m].

2.3. Model configurations

In the previous sections, the SWAN-model was introduced. It was stated that simulated results from this model would be compared with observational data. To obtain accurate and reliable simulational results, it is important to configure the model appropriately.

Since the underlying physics for the SWAN-model is to a large extent founded in empirical formulations, many commands that control model physics have parameters that can be chosen to differ from a default value. Naturally, this freedom in choosing model parameters expands the parameter space in which simulations can be performed and compared. This project will not be concerned with configuring parameters for the Haringvliet bathymetry. Instead, default parameters will be adopted throughout the computations.

A problem arises when comparing results with observational data, which is sampled linearly between 0 and 1 [Hz] with increments of 0.01 [Hz], while the SWAN-data is sampled logarithmically (in this project: between 0.0521 [Hz] and 1 [Hz] with the total number of sample points being 32). Because of the logarithmic distribution of frequency points in SWAN, it is not possible to request a frequency output that matches exactly the frequency distribution of the observational data. Therefore, we resort to downsampling of the observed data such that interpolated values are available at the same points in the frequency domain as the SWAN-data using `scipy.interpolate.interp1d()`.

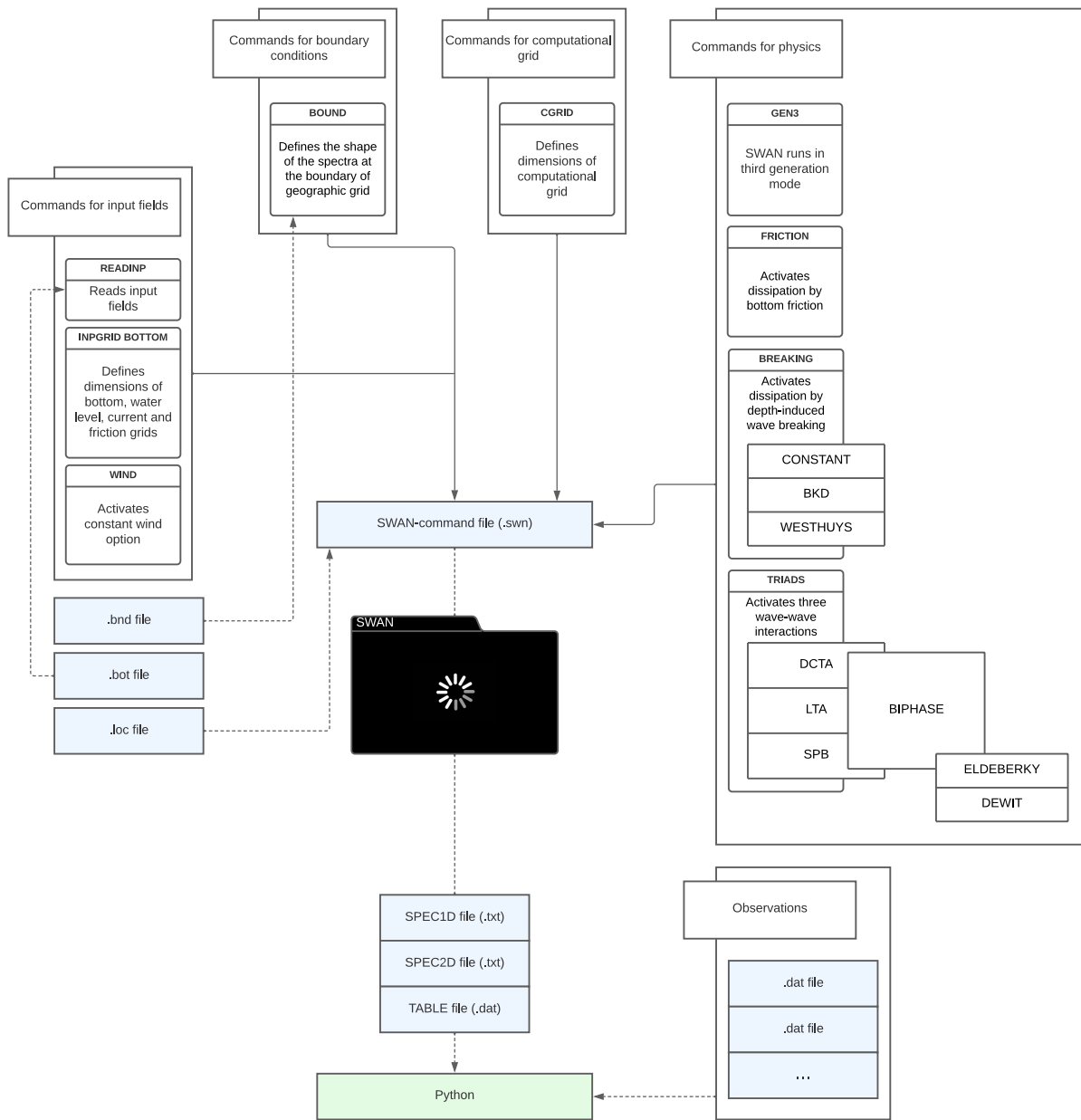


Figure 2.1: Schematic of the pipeline used to simulate and process data. Details of the SWAN-commands on display can be found in Fluidmechanics Section, Delft University of Technology (2023b). Technical details and background on SWAN can be found in Fluidmechanics Section, Delft University of Technology (2023a). Configuration options for the commands have been omitted, with exception of some parameters under BREAKING and TRIADS because of the significance for this project. Input/output files are indicated by blue boxes. Details concerning the SWAN-command file setup, external input and Python code are available upon request. Own work.

3

Discussion of results

3.1. General remarks

Figure 3.1 provides a side-by-side comparison of the observational spectra and simulated spectra that include the effect of wave breaking. The wave breaking formulations that are compared are BKD, CONSTANT and WESTHUYSEN. Locations correspond to Figure 1.2. At first glance, three features come to attention:

- The simulations are effective at reproducing the location of the spectral peak in the case of location 1, 2 and 3 (before breaking) and location 6 (after breaking);
- The spectrum at location 5 (after breaking) looks decidedly more jagged than the other spectra and features multiple peaks. Also, it is more ambiguous whether the simulations manage to reproduce the central peak;
- The magnitude of the observational data at Location 4, 23:10 UTC, is much lower than the magnitude of the simulated spectra. Contrary to other observational spectra, it also shows no defined peak. Careful inspection of the measurement files reveals that this is a feature inherent to the data rather than an issue with the processing. Another dataset that is available to us at location 4, measured at 22:50 UTC shows similar characteristics. This implies that either the observational data at location 4 is flawed, or the simulations are way off at this point. Note that simulated results at location 4 are almost (but not quite) identical to the results at location 3, which makes sense since these are both located at close proximity and before the shoal.

The second feature is especially relevant for this project, since it reinforces our motivation for investigating a possible frequency dependence in the wave breaking process. Figure C.1 and C.2 also show two-dimensional spectra without and with the effect of wave breaking (using the CONSTANT-formulation) to provide an opportunity for visualization and for a qualitative comparison of breaking effects.

3.2. Assessment of interpolation effects

To exclude the possibility that the relative shift in the peak location and the difference in amplitude that are apparent in Figure 3.1 is an unwanted side-effect of the resampling process, we first assess the performance of resampling and subsequently interpolating the observational spectra. Figure 3.2 shows observed and interpolated spectra for location 4 and 5. The general shape agrees well, although some loss of information is inevitable since the rate of resampling follows a log spacing and is therefore lower at the high frequency end of the spectrum. To quantify the difference between original and resampled spectra, we numerically evaluate the spectral power (integrated energy density) using the `integrate.cumtrapz()`-method from Scipy. This yields quantities E_0 for the power of the original spectrum and E_r for the power of the resampled spectrum. Figure 3.3 visualizes the relation between E_0 and E_r . Table 3.1 provides the ratio E_0/E_r for each location/timestamp pair. It is found that E_0/E_r is close to 1 for all pairs. In a similar fashion, the relative peak shift is derived. The ratio $f_{p,r}/f_{p,0}$ is found to be close to 1 except for location 4 at 23:10 UTC. We already commented on the divergent shape of the observational data at location 4 in Section 3.1 and neglect this effect for the time being.

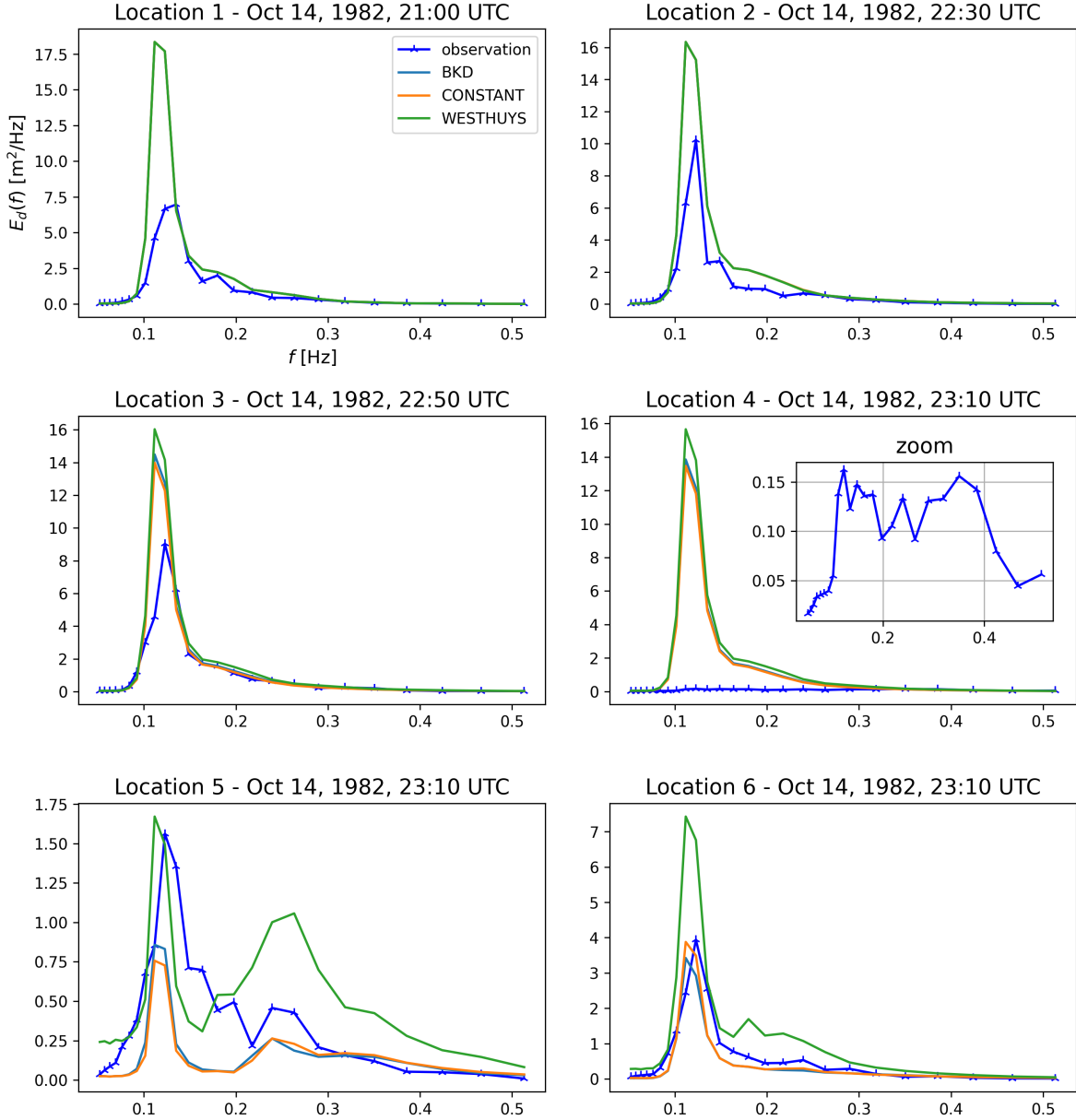


Figure 3.1: Observed spectra and simulated spectra at six locations indicated in Figure 1.2. Date and time in the figure caption refers to the timestamp of the measurement data (the observed spectra) with respect to UTC.

We conclude that resampling and interpolation of the data preserves the spectral energy and does not pose problems for the remaining part of the analysis.

3.3. Dissipation coefficients

Figure 3.4 shows the dissipation coefficients for the trajectories 4-5 (α_1) and 3-6 (α_2) as calculated using equation (2.1) and (2.2). The dissipation coefficient shows a clear dependency on frequency for α_1 , but not so for α_2 . Specifically, the increase in dissipation for α_1 is exceptionally pronounced at lower frequencies. This is an indication that the assumption of constant frequency dependence in the breaker formulations is unjustified. The inset of Figure 3.4 shows the same results plotted on a log scale to emphasize small fluctuations. An important remark here is that the computation of α_1 relies on $S_{meas,4}$ in the denominator. In Section 3.1 and 3.2, we discussed some issues with $S_{meas,4}$ that makes it hard to tell whether this spectrum is at all reliable. In the remained of the analysis, we will assume

Table 3.1: Power in the resampled spectrum (E_r) as a fraction of power in the original spectrum (E_0) for observational data on six locations with various timestamps. Numbers are rounded to 2 decimals. Ratios are close to 1 indicating that no significant information loss is incurred through the resampling procedure. Figure 3.3 shows the values of E_r and E_0 for each measurement.

[Location],[timestamp]	E_r/E_0	$f_{p,r}/f_{p,0}$
L1,01:30	1.00	0.02
L1,21:00	1.00	0.04
L2,00:00	1.00	0.02
L2,22:30	1.03	0.02
L3,22:50	0.99	0.02
L4,22:50	0.99	0.00
L4,23:10	1.00	-0.68
L5,22:50	0.99	-0.06
L5,23:10	1.03	0.02
L6,21:40	1.06	0.04
L6,23:10	1.03	0.02

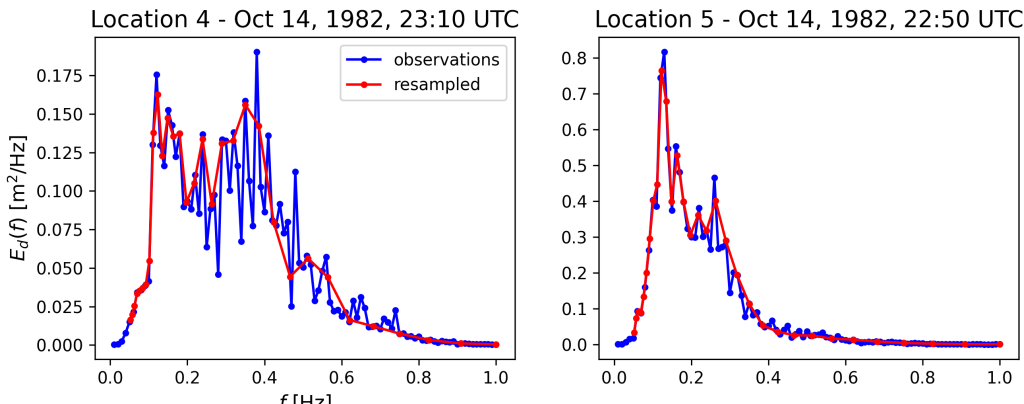


Figure 3.2: Observed and interpolated spectra for location 4 and 5. The resampling procedure and subsequent interpolation preserves the general shape of the spectrum with some loss of detail since the resampling rate is lower at high frequencies.

the spectrum is reliable. In the conclusion, we discuss the implications of this assumption and suggest a course of action for future research.

In order to state whether there is a statistically significant frequency dependence in the dissipation coefficient, the Kendall's tau coefficient is computed for α_1 and α_2 and a z-test is performed. Details on the statistical test are provided in Appendix B. For our problem, the zero hypothesis H_0 states that there exists no (frequency-dependent) trend in the dissipation coefficient; the alternative hypothesis H_a then states that there exists such a trend in the dissipation coefficient. For a 0.05 significance level with a two-tailed z-test, the critical values are ± 1.96 . It is found that α_1 has a Kendall's tau coefficient of -0.46 and a value of the test statistic $z_A = -3.22$, while α_1 has a tau coefficient of 0.047 and $z_A = 0.33$. Consequently, for α_1 , H_0 is rejected in favour of H_a ; for α_2 , H_0 is not rejected.

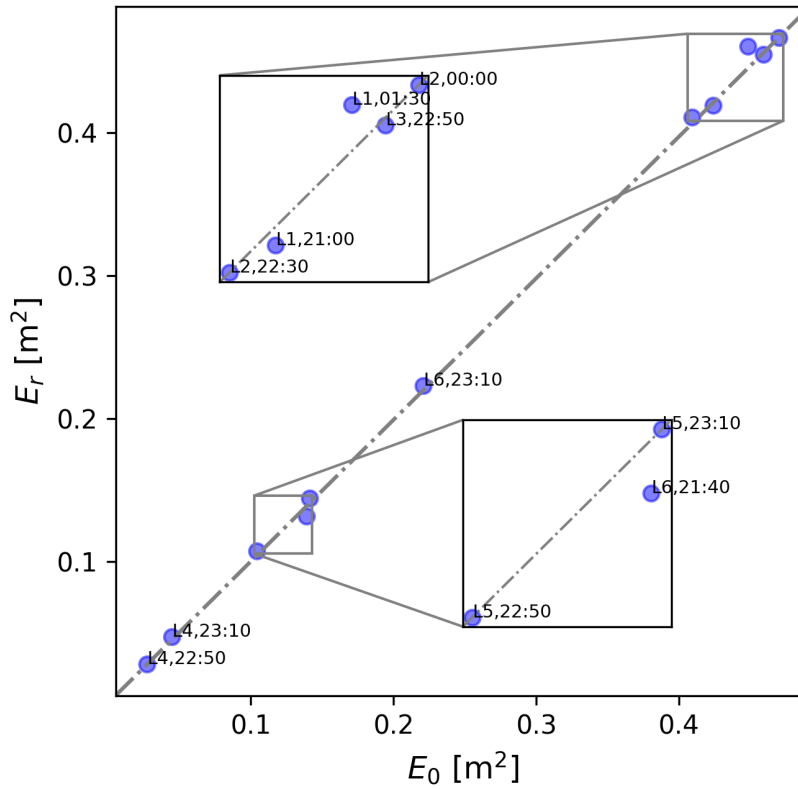


Figure 3.3: Integrated spectral power for the original observed spectra (E_0) and the resampled observed spectra (E_r). Points on the dotted line sustain no net loss of spectral power. Labels represent measurement location and timestamp with the syntax [Location],[timestamp]. The figure suggests that the interpolation procedure preserves important characteristics of the spectra.

This agrees with Figure 3.2. Ratios E_r/E_0 are given in Table 3.1.

3.4. Comparison of dissipation coefficients with Chen et al. (1997), Kuznetsov and Saprykina (2004) and Meza et al. (2002)

Figure 3.5 shows observational spectra together with the predicted dissipation S_{dis} according to Meza et al. (2002). To improve readability and provide a general feeling for the characteristic behaviour of S_{dis} , averaged values are displayed in the inset. Needless to say, this approach is rather hand-wavy since the various curves represent data at different locations and are therefore not realizations of the same random variable; it is the general shape that matters here. From comparison with Figure 3.4, it is evident that the agreement between predicted S_{dis} and dissipation coefficients α_1 and α_2 is poor. Calculated dissipation coefficients show significant accumulation of energy loss at higher frequencies, while predicted S_{dis} shows dissipation mainly at frequencies higher than the peak frequency and a small energy gain at frequencies below the peak, as discussed in Section 1.3. One reason for this discrepancy might be the highly non-unidirectional nature of the wave spectra in the Haringvliet compared to the unidirectional transient wave trains that were created under laboratory-controlled circumstances to underpin the arguments outlined in Meza et al. (2002), Meza et al. (2000).

The dissipation coefficients do not tend towards high frequencies as predicted by Chen et al. (1997), and neither do they agree with the quadratic frequency dependence proposed by Kuznetsov and Saprykina (2004). A likely reason for this is again the questionable quality of the observations at location 4, as discussed in Section 3.1 and 3.2.

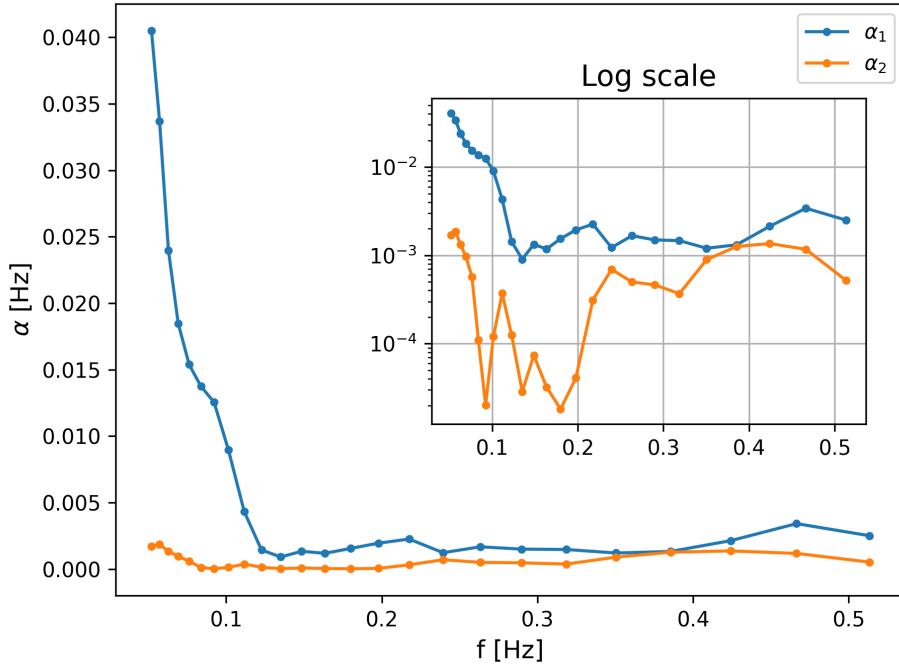


Figure 3.4: α_1 and α_2 for the DCTA formulation with the biphasic evolution of ELDEBERKY, according to equation (2.1) and (2.2). The inset shows the same data on logarithmic scale to accentuate the differences. For α_1 , a Kendall's tau coefficient of -0.46 and a p-value of is found. For α_2 , the values are 0.047 and respectively. Note the strong apparent frequency dependence of α_1 .

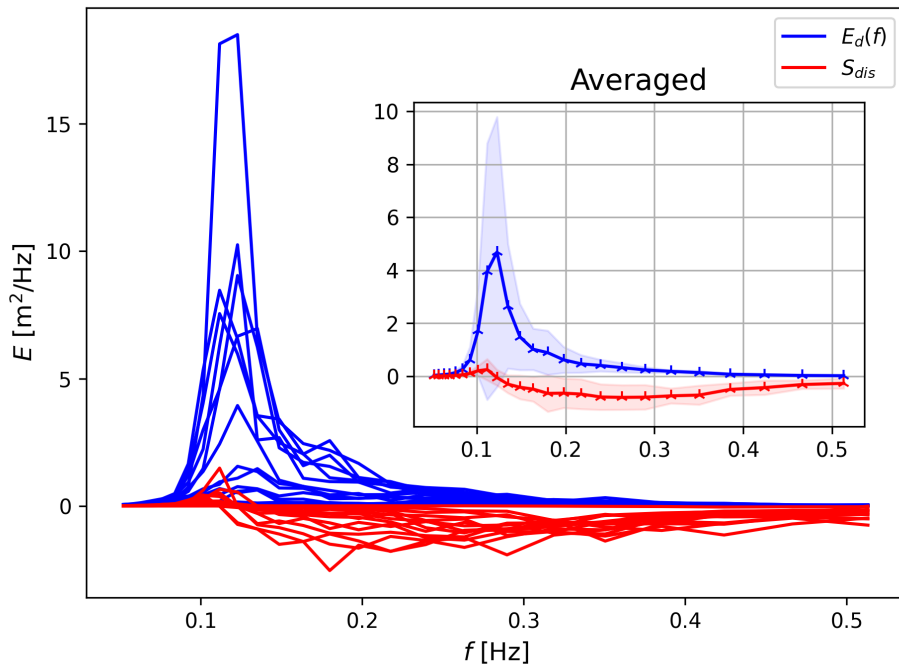


Figure 3.5: Observational spectra and predicted dissipation S_{dis} according to Meza et al. (2002). In the inset, the multitude of curves has been averaged to produce an indication of the characteristic behaviour. Shaded areas represent the first standard deviation confidence interval.

4

Conclusion and outlook

In this project, observational results from the Hinderplaat shoal in the Haringvliet estuary (Netherlands) were compared with wave spectra that were generated in SWAN. Specifically, the dissipation coefficient was computed over two trajectories traversing the Hinderplaat shoal. A z-test based on Kendall's tau coefficient revealed a statistically significant trend in the frequency dependence of the dissipation coefficient for one of the two trajectories at a significance level of 0.05. Based on these results alone, it is anticipated that the wave breaker formulations would benefit from some form of adjustment to account for frequency-dependent effects. It was however remarked that the dissipation coefficient with a frequency dependence relies on an observational spectrum of questionable quality: its magnitude does not agree at all with observational data at neighbouring sites, it shows no defined peak and it shares none of the characteristics of simulated results at the same location. This effectively makes it impossible to reliably attribute the observed frequency dependence in the dissipation coefficient to a physical process.

For future efforts on this topic, it is recommended that the following course of action be taken. First of all, the quality of the conclusion would increase if a study on another test site were conducted. The best choice for a test site is a similar shoal-estuary system, since this would pose the least difficulties for comparing outcomes. Potential shoal-estuary systems which are likely to boast a decent level of documentation are the Thames and Gironde estuary in Europe and the San Francisco Bay area in the USA. Depending on a comparison of outcomes, the next course of action could be to conduct a theoretical review of the wave breaking formulations presented in this report and to propose a suitable modification.

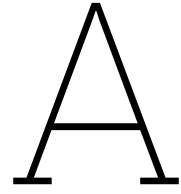
In the process of setting up the simulations in the limited time available for the project, no priority was given to the tuning of physics commands in order to best resemble the situation in the Haringvliet estuary. As a consequence, most of the calibration parameters in SWAN have been assigned their default values and are therefore sub-optimally configured. To improve the quality of the results, a thorough calibration is desirable for any follow-up research.

Lastly, it is suggested to simulate the breaking process with a broader variety of parametrizations for the nonlinear triad interactions. In this context, the recent parametrization for the biphase evolution of DEWIT is mentioned. Originally, it was the intent of the author to conduct the simulations in SWAN using this parametrization; due to difficulties during implementation, a change was made to EIDEBERKY.

Bibliography

- Abdi, H. (2007). The kendall rank correlation coefficient. *Encyclopedia of Measurement and Statistics*. Sage, Thousand Oaks, CA, 508–510.
- Battjes, J., & Janssen, H. (1978). Energy loss and set-up due to breaking random waves. *Proceedings of the 16th International Conference on Coastal Engineering*, 1. <https://doi.org/10.9753/icce.v16>
- Battjes, J., & Stive, M. (1985). Calibration and verification of a dissipation model for random breaking waves. *Journal of Geophysical Research* 90(C5), 9159-9167. (1985), 90. <https://doi.org/10.1029/JC090iC05p09159>
- Becq-Girard, F., Forget, P., & Benoit, M. (1999). Non-linear propagation of unidirectional wave fields over varying topography. *Coastal Engineering*, 38(2), 91–113. [https://doi.org/10.1016/S0378-3839\(99\)00043-5](https://doi.org/10.1016/S0378-3839(99)00043-5)
- Beji, S., & Battjes, J. (1993). Experimental investigation of wave propagation over a bar. *Coastal Engineering*, 19(1), 151–162. [https://doi.org/10.1016/0378-3839\(93\)90022-Z](https://doi.org/10.1016/0378-3839(93)90022-Z)
- Bonett, D. G., & Wright, T. A. (2000). Sample size requirements for estimating pearson, kendall and spearman correlations. *Psychometrika*, 65, 23–28.
- Booij, N., Holthuijsen, L., & Bénit, M. P. (2009). A distributed collinear triad approximation in swan. In *Proceedings of coastal dynamics 2009* (pp. 1–10). https://doi.org/10.1142/9789814282475_0006
- Chen, Y., Guza, R., & Elgar, S. (1997). Modeling spectra of breaking surface waves in shallow water. *Journal of Geophysical Research: Oceans*, 102(C11), 25035–25046.
- Chen, Y., & Liu, P. L.-F. (1995). Modified boussinesq equations and associated parabolic models for water wave propagation. *Journal of Fluid Mechanics*, 288, 351–381.
- de Wit, F. (2022). *Wave shape prediction in complex coastal systems* (Doctoral dissertation). Delft University of Technology, Department of Civil Engineering. Delft, The Netherlands.
- Durant, T., Johnson, D., Ströfer, C., Rapizo, H., Harrington, J., Perez, J., Branson, P., de Brujin, R., Coe, R., & Bak, S. (2023). Wavespectra. Retrieved February 27, 2023, from <https://wavespectra.readthedocs.io/en/latest/index.html>
- Eldeberky, Y. (1996). *Nonlinear transformation of wave spectra in the nearshore zone* (Doctoral dissertation). Delft University of Technology, Department of Civil Engineering. Delft, The Netherlands.
- European Space Agency. (2020). Applications: Zeeland, Netherlands. https://www.esa.int/ESA_Multimedia/Images/2020/10/Zeeland_Netherlands
- Fluidmechanics Section, Delft University of Technology. (n.d.). Welcome to the SWAN home page. Retrieved February 27, 2023, from <https://swanmodel.sourceforge.io/>
- Fluidmechanics Section, Delft University of Technology. (2023a). Scientific and technical documentation. Retrieved February 27, 2023, from https://swanmodel.sourceforge.io/online_doc/swantech/swantech.html
- Fluidmechanics Section, Delft University of Technology. (2023b). User manual. Retrieved February 27, 2023, from https://swanmodel.sourceforge.io/online_doc/swanuse/swanuse.html
- Hasselmann, K. (1971). On the mass and momentum transfer between short gravity waves and larger-scale motions. *Journal of Fluid Mechanics*, 50(1), 189–205.
- Kendall, M. G. (1938). A new measure of rank correlation. *Biometrika*, 30(1/2), 81–93.
- Kuznetsov, S. Y., & Saprykina, Y. V. (2004). Frequency-dependent energy dissipation of irregular breaking waves. *Water resources*, 31, 384–392.
- Longuet-Higgins, M. S. (1969). A nonlinear mechanism for the generation of sea waves. *Proceedings of the Royal Society of London. A. Mathematical and Physical Sciences*, 311(1506), 371–389.
- Melville, W. K. (1996). The role of surface-wave breaking in air-sea interaction. *Annual review of fluid mechanics*, 28(1), 279–321.
- Meza, E., Zhang, J., Olivares, A., & Brambila, J. (2002). *Third Generation Wind Wave Model Frequency Dependence of the White-Capping Dissipation Source Function* (Vol. 21st International Con-

- ference on Offshore Mechanics and Arctic Engineering, Volume 4). <https://doi.org/10.1115/OMAE2002-28051>
- Meza, E., Zhang, J., & Seymour, R. J. (2000). Free-wave energy dissipation in experimental breaking waves. *Journal of Physical Oceanography*, 30(9), 2404–2418. [https://doi.org/https://doi.org/10.1175/1520-0485\(2000\)030<2404:FWEDIE>2.0.CO;2](https://doi.org/https://doi.org/10.1175/1520-0485(2000)030<2404:FWEDIE>2.0.CO;2)
- Puleo, J., Beach, R., Holman, R. A., & Allen, J. (2000). Swash zone sediment suspension and transport and the importance of bore-generated turbulence. *Journal of Geophysical Research: Oceans*, 105(C7), 17021–17044.
- Rapp, R., & Melville, W. (1990). Laboratory measurements of deep-water breaking waves. *Royal Society of London Philosophical Transactions Series A*, 331, 735–800. <https://doi.org/10.1098/rsta.1990.0098>
- Ris, R., Booij, N., & Holthuijsen, L. (1999). A third-generation wave model for coastal regions: 2. verification. *J. Geophys. Res.*, 104, 7667–7681. <https://doi.org/10.1029/1998JC900123>
- Salmon, J. E. (2016). *Surf wave hydrodynamics in the coastal environment* (Doctoral dissertation). Delft University of Technology, Department of Civil Engineering. Delft, The Netherlands.
- Salmon, J., & Holthuijsen, L. (2015). Modeling depth-induced wave breaking over complex coastal bathymetries. *Coastal Engineering*, 105, 21–35. <https://doi.org/10.1016/j.coastaleng.2015.08.002>
- Salmon, J., Holthuijsen, L., Zijlema, M., van Vledder, G., & Pietrzak, J. (2015). Scaling depth-induced wave-breaking in two-dimensional spectral wave models. *Ocean Modelling*, 87, 30–47. <https://doi.org/https://doi.org/10.1016/j.ocemod.2014.12.011>
- Saprykina, Y., Aydoğan, B., & Ayat, B. (2022). Wave energy dissipation of spilling and plunging breaking waves in spectral models. *Journal of Marine Science and Engineering*, 10, 200. <https://doi.org/10.3390/jmse10020200>
- Van der Westhuysen, A. J. (2009). Modelling of depth-induced wave breaking over sloping and horizontal beds. *Proc. 11th International Workshop on Wave Hindcasting and Forecasting*.
- Westhuysen, A. (2010). Modeling of depth-induced wave breaking under finite depth wave growth conditions. *Journal of Geophysical Research (Oceans)*, 115. <https://doi.org/10.1029/2009JC005433>
- Whitford, D. J. (1988). *Wind and wave forcing of longshore currents across a barred beach*. Naval Postgraduate School.
- Wikimedia Commons. (2015). Types of breaking waves on slopes: Spilling, plunging, collapsing and surging. Retrieved March 12, 2023, from https://commons.wikimedia.org/wiki/File:Breaking_wave_types.svg
- Wright, L. D., & Short, A. D. (1984). Morphodynamic variability of surf zones and beaches: A synthesis. *Marine geology*, 56(1-4), 93–118.
- Xi advies bv. (n.d.). f031harin[001-004]: Haringvliet estuary (the Netherlands). <http://demo.xi-alles.nl/swift/references/f031harin.pdf>



Source Code

The following code block gives an impression of the contents from the SWAN-command files that were used to run some of the simulations. For the general structure of the command file, see Figure 2.1.

```
1 $*****HEADING*****
2 $
3 PROJ 'F31har04' 'F31'
4 $
5 $ Field case: The Haringvliet test 4 of 4
6 $ test 1 Time of simulation: 21:00 UTC on October 14, 1982
7 $ test 2 Time of simulation: 22:00 UTC on October 14, 1982
8 $ test 3 Time of simulation: 23:00 UTC on October 14, 1982
9 $ test 4 Time of simulation: 24:00 UTC on October 14, 1982
10 $
11 $ Date of simulation: 24:00 UTC
12 $
13 $ WL    = + 2.10
14 $ Hs    = 3.53 m
15 $ Tm01 = 6.9 s
16 $ Tp    = 8.3 s
17 $
18 $ --|-----|--
19 $ | This SWAN input file is part of the bench mark tests for |
20 $ | SWAN. More information about this test can be found in   |
21 $ | an accompanied document.                                |
22 $ --|-----|--
23 $*****MODEL INPUT*****
24 SET LEVEL 2.10
25 $
26 CGRID 6960.2 0. 0. 14789.8 22000. 98 88 CIRCLE 36 0.0521 1. 31
27 $
28 INPGRID BOTTOM 0. 0. 0. 87 116 250. 250. EXC -7.0
29 READINP BOTTOM .1 'f31hari.bot' 1 6 FORMAT 1
30 $
31 WIND 15. 8.8
32 $
33 BOU SIDE W CCW CON FILE 'f31har04.bnd' 1
34 $
35 GEN3 WESTH DRAG WU
36 FRICT
37 BREAK WESTH
38 TRIADS BIPHASE ELD 0.2
39 $
40 $*****POINTS 'BUOYS' FILE 'f31hari.loc'
41 TABLE 'BUOYS' HEAD 'f31har04.tab' DIST DEP HS RTP TM01 TM02 FSPR DIR SETUP
42 SPEC 'BUOYS' SPEC1D 'westh.spc'
43 $
44 $
45 TEST 1,0
46 COMPUTE
47 STOP
```

B

Some background on statistical testing with Kendall's tau coefficient for α_1 and α_2

This appendix aims to provide some background on the method for computing Kendall's tau coefficient (alternatively called the Kendall rank correlation coefficient) for α_1 and α_2 and the method for statistical verification of frequency independence. We commence by defining a null hypothesis and an alternative hypothesis for the problem:

- H_0 : there exists no dependence of the dissipation coefficient on frequency;
- H_a : there exists a dependence of the dissipation coefficient on frequency.

To decide on H_0 or H_a , we need to perform a statistical test. For reasons that are outlined below, a test based on Kendall's tau coefficient (Kendall, 1938) suits our needs. A statistical test based on Pearson's correlation coefficient would be inappropriate because it is a measure of strength for the linear relationship between variables and we don't know *a priori* what relationship (if any) we should expect. Alternatively, a test based on Spearman correlation could be performed, but since our sample size is fairly small a Kendall test is preferred (Bonett & Wright, 2000). Kendall's tau coefficient measures the ordinal (rank based) association between two quantities. For the purpose of this project, the τ_A statistic is chosen. The τ_A statistic does not adjust for ties (a pair $\{(x_i, x_j), (y_i, y_j)\}$ of observations of the joint random variables X and Y is called *tied* if $x_i = x_j$ or $y_i = y_j$); however, we do not expect this to be a problem since we defined our frequency array to be linear (no repeating values) and the array with values for the dissipation coefficient can be seen to be non-repetitive just by looking at it. τ_A is defined as follows:

$$\tau_A = \frac{n_c - n_d}{n_0} \quad (\text{B.1})$$

Here, $n_0 = n(n - 1)/2$ with n representing the total number of observations in the sample. n_c and n_d represent the number of *concordant* and *discordant* pairs respectively. Any pair of observations $\{(x_i, x_j), (y_i, y_j)\}$ with $i < j$ is said to be concordant if both $x_i > x_j$ and $y_i > y_j$ or both $x_i < x_j$ and $y_i < y_j$ (*i.e.* the sort order agrees). Similarly, any pair of observations is said to be discordant if $x_i > x_j$ and $y_i < y_j$ or $x_i < x_j$ and $y_i > y_j$. It is known that for statistically independent variables, the statistic

$$z_A = \frac{3\sqrt{2}(n_c - n_d)}{\sqrt{n(n - 1)(2n + 5)}} = \frac{3\tau_A\sqrt{n(n - 1)}}{\sqrt{2(2n + 5)}} \quad (\text{B.2})$$

is approximately normally distributed with mean 0 and variance 1 (Abdi, 2007). Hence, we can use z_A as the test statistic for a two-tailed test. Using a significance level of 0.05, the corresponding critical values for z_A are easily found from a table: $z_{A,c} = \pm 1.96$. If $|z_A| > |z_{A,c}|$, H_0 is rejected.

Computing the number of concordant and discordant pairs is possible with a nested loop. The code snippet below shows a possible approach to this problem. Here, `frequencies` represents the array with frequency values and `alpha` represents the array with values for the dissipation coefficient at these frequencies. After n_c and n_d have been obtained, finding τ_A and z_A is trivial.

```

1 nc = 0
2 nd = 0
3 for i in range(len(frequencies)):
4     for j in range(i+1, len(frequencies)):
5         if ((frequencies[i] < frequencies[j]) & (alpha[i] < alpha[j]) | (frequencies[i] >
6             frequencies[j]) & (alpha[i] > alpha[j])):
7             nc += 1
8         elif (frequencies[i] < frequencies[j]) & (alpha[i] > alpha[j]):
9             nd += 1
10 n      = len(frequencies)
11 tau_A  = (nc - nd)/(n*(n-1)/2)
12 z_A    = (3*tau_A*np.sqrt(n*(n-1)))/(np.sqrt(2*(2*n+5)))

```

C

Simulated results: frequency-direction spectral plots

To give a qualitative insight into the simulated results, Figure C.1 shows the two-dimensional, modelled wave spectra at locations 3 and 4 (in front of the Hinderplaat) and 5 and 6 (behind the Hinderplaat). Comparing these figures, it is worth noting that for the modelled spectra, the spectral energy flows from lower to higher frequencies over the Hinderplaat. This behaviour agrees partly with the course of α_1 which shows high dissipation at low frequencies. However, α_1 does not replicate the gain in energies at higher frequencies that emerges from the modelled 2D-spectra when comparing location 3 with location 6 or location 4 with location 5. It is reasonable that the modelled spectra fail to capture this aspect, since they *exclude* the contribution of wave breaking. In contrast, Figure C.2 shows the two-dimensional spectra where the CONSTANT-breaking formulation has been included. Here, a clear reduction in spectral energy is visible at locations behind the Hinderplaat.

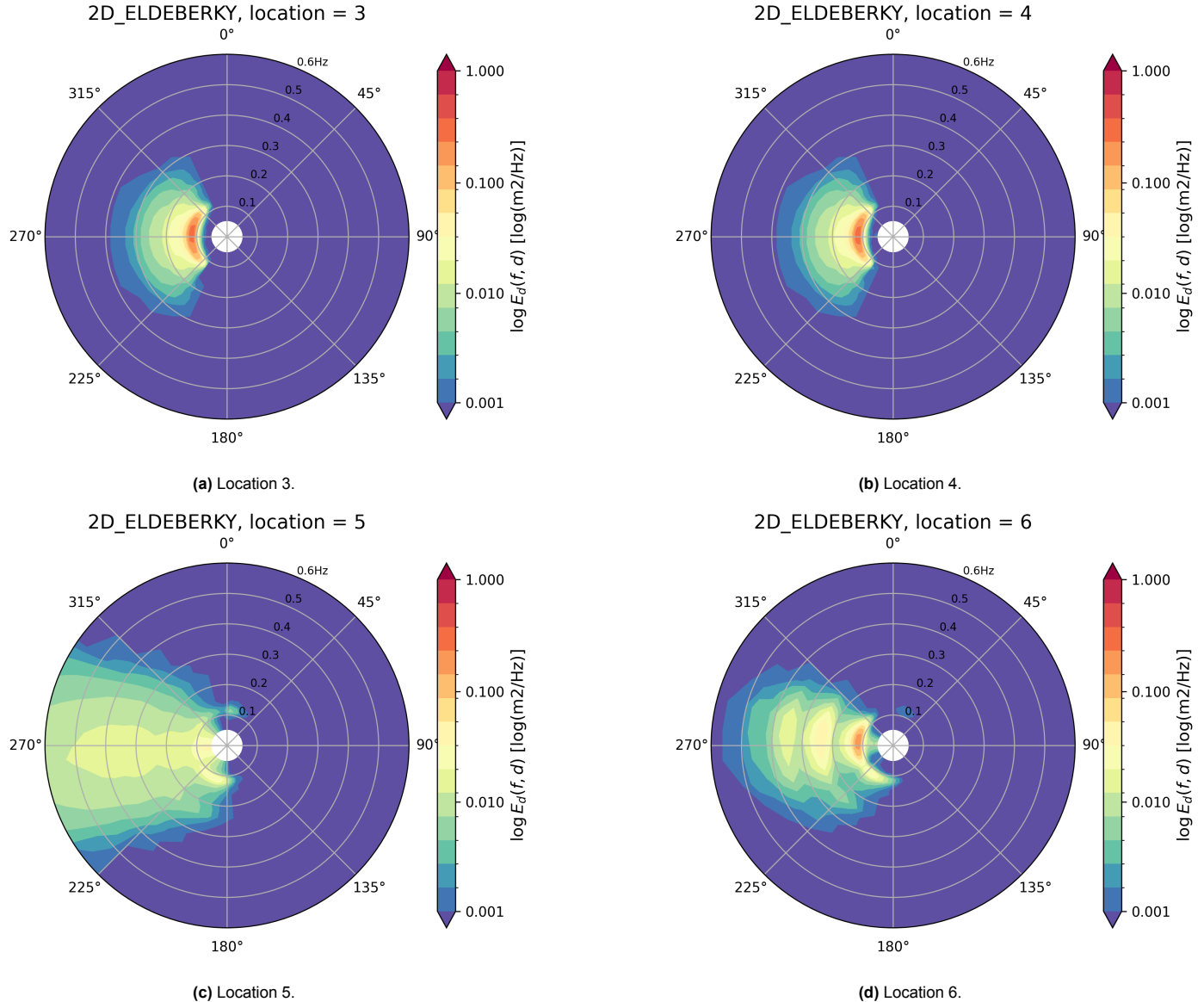


Figure C.1: 2-dimensional, (non-normalized) wavespectra at locations 3, 4, 5 and 6, excluding the contribution of breaking terms.

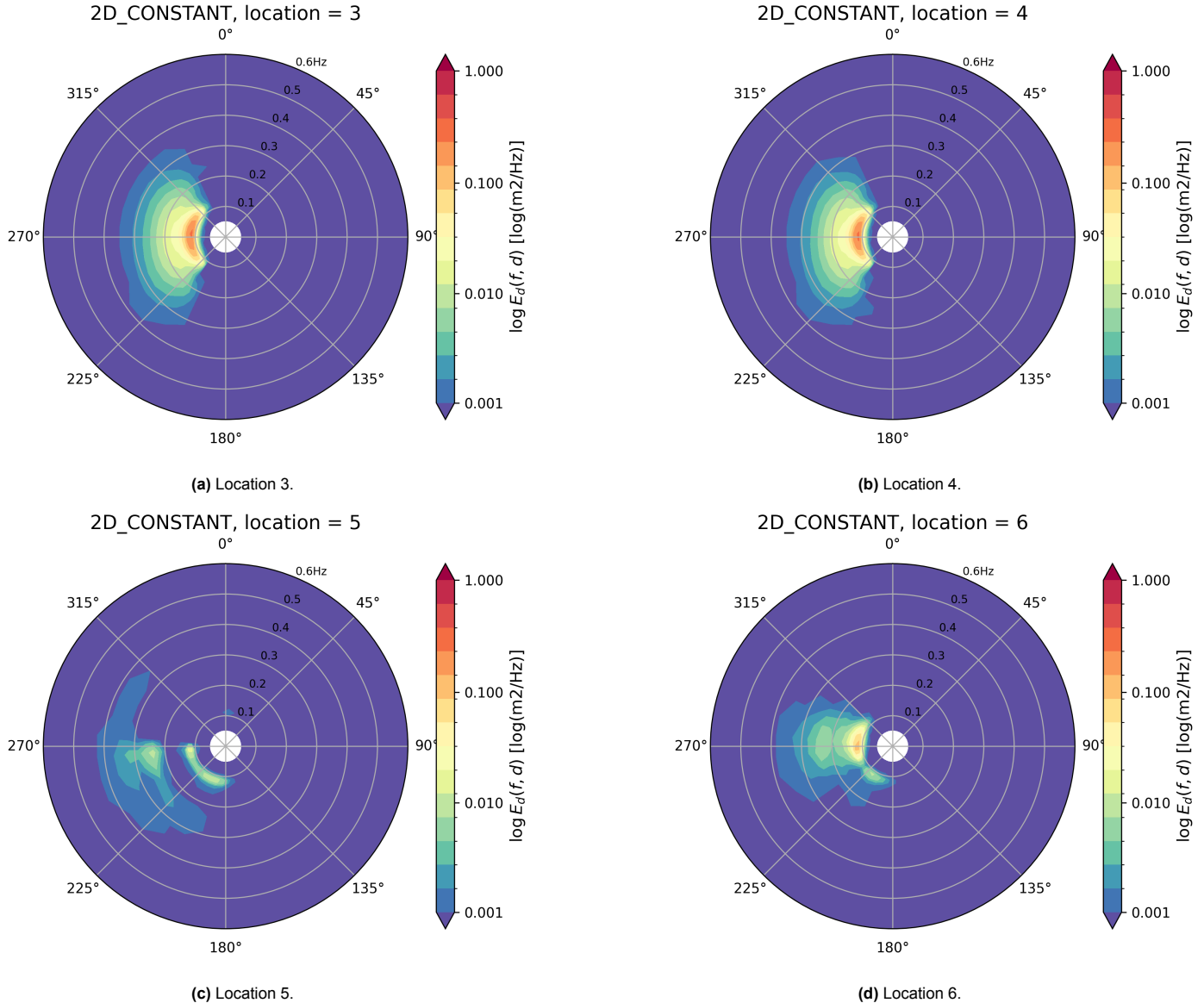


Figure C.2: 2-dimensional, (non-normalized) wavespectra at locations 3, 4, 5 and 6, including the contribution of breaking terms (with the CONSTANT-breaking formulation).

D

Interim evaluation: roadmap and peer review

This appendix includes the peer review for the interim report ('tussenrapport') and presentation ('tussenvresentatie') by student Paul Thönissen as a reference for the evaluation of the final report. It also includes the initial roadmap for the project ('startnotitie'). Note that the descriptions offered in the startnotitie do not provide an accurate representation for the structure of the final report, since the project has developed in a much more organic manner than was originally expected.

Rapport van: Matthijs Wanrooij

Titel: Performance of wave breaker formulations in SWAN

Datum: 9-3-2023

Naam reviewer Paul Thönissen

Hieronder staat een aantal uitspraken over verschillende aspecten van de rapportage. Geef aan in hoeverre u het met deze uitspraken eens bent. Bij de presentatie kan u gevraagd worden uw waardering te onderbouwen!

De volgende schaal wordt gebruikt:

- 1 = zeer mee oneens
- 2 = overwegend oneens
- 3 = niet zeker
- 4 = overwegend eens
- 5 = zeer mee eens

Rapport	1	2	3	4	5
1. Het rapport heeft een heldere opbouw.	<input type="checkbox"/>	<input type="checkbox"/>	<input type="checkbox"/>	<input checked="" type="checkbox"/>	<input type="checkbox"/>
2. Er is voldoende gebruik gemaakt van de beschikbare vakliteratuur.	<input type="checkbox"/>	<input type="checkbox"/>	<input type="checkbox"/>	<input type="checkbox"/>	<input checked="" type="checkbox"/>
3. De literatuurverwijzingen in de tekst van het rapport zijn volgens de regels.	<input type="checkbox"/>	<input type="checkbox"/>	<input type="checkbox"/>	<input type="checkbox"/>	<input checked="" type="checkbox"/>
4. Het rapport geeft de belangrijkste aspecten van het onderwerp voldoende weer.	<input type="checkbox"/>	<input type="checkbox"/>	<input type="checkbox"/>	<input checked="" type="checkbox"/>	<input type="checkbox"/>
5. Uit het rapport wordt goed duidelijk wat het uiteindelijke ontwerp / conclusie is.	<input type="checkbox"/>	<input type="checkbox"/>	<input checked="" type="checkbox"/>	<input type="checkbox"/>	<input type="checkbox"/>
6. Na lezing van het rapport is mij duidelijk geworden waar mijn eigen rapport beter kan.	<input type="checkbox"/>	<input type="checkbox"/>	<input type="checkbox"/>	<input checked="" type="checkbox"/>	<input type="checkbox"/>
7. Het rapport leest plezierig.	<input type="checkbox"/>	<input checked="" type="checkbox"/>	<input type="checkbox"/>	<input type="checkbox"/>	<input type="checkbox"/>
Alleen voor het eindrapport invullen als je ook het tussenrapport hebt beoordeeld: 8. Het eindrapport is beter dan het tussenrapport.	<input type="checkbox"/>	<input type="checkbox"/>	<input type="checkbox"/>	<input type="checkbox"/>	<input type="checkbox"/>

**Gebruik deze ruimte voor een korte beschouwing over het rapport
(ongeveer 150 tot 200 woorden).**

Het rapport is over het algemeen zeer professioneel geschreven. De opmaak ziet er goed uit, de bronvermelding is geheel volgens de regels, het taalgebruik is op niveau en er wordt goed gebruik gemaakt van vakliteratuur. Je maakt ook goed gebruik van SWAN en Python, dit voegt echt wat toe aan je onderzoek.

Aan de andere kant is het niveau misschien iets te hoog en ga je iets te diep op de materie in. Sommige stukken moest ik wel drie keer lezen om het te kunnen begrijpen en er wordt veel gebruik gemaakt van vaktermen, afkortingen en formules, wat het lezen ook niet makkelijker maakt.

In de introductie kan je misschien iets rustiger op de materie ingaan door eerst wat meer achtergrondinformatie te geven voor je de diepte in gaat.

Misschien is het een idee om in een figuur aan te geven waar het gebied is wat je bekijkt, ik heb persoonlijk weleens van de Haringvliet gehoord maar weet ook niet precies waar het is.

Presentatie van: Matthijs Wanrooij

Titel: Performance of wave breaker formulations in SWAN

Datum: 10-3-2023

Naam reviewer Paul Thönissen

Hieronder staat een aantal uitspraken over verschillende aspecten van de presentatie. Geef aan in hoeverre u het met deze uitspraken eens bent.

De volgende schaal wordt gebruikt:

- 1 = zeer mee oneens
- 2 = overwegend oneens
- 3 = niet zeker
- 4 = overwegend eens
- 5 = zeer mee eens

Presentatie	1	2	3	4	5
1. De presentatie heeft een heldere opbouw.	<input type="checkbox"/>	X	<input type="checkbox"/>	<input type="checkbox"/>	<input type="checkbox"/>
2. Formules worden niet gebruikt of duidelijk gedefinieerd	<input type="checkbox"/>	X	<input type="checkbox"/>	<input type="checkbox"/>	<input type="checkbox"/>
3. De methode is duidelijk samengevat.	X	<input type="checkbox"/>	<input type="checkbox"/>	<input type="checkbox"/>	<input type="checkbox"/>
4. De resultaten zijn samengevat in adequate grafieken, schema's, tabellen en tekeningen	X	<input type="checkbox"/>	<input type="checkbox"/>	<input type="checkbox"/>	<input type="checkbox"/>
5. Alle getallen, astitels, bijschriften etc. zijn duidelijk leesbaar en volledig (inclusief eenheden)	X	<input type="checkbox"/>	<input type="checkbox"/>	<input type="checkbox"/>	<input type="checkbox"/>
6. Na het zien van de presentatie is mij duidelijk geworden waar mijn eigen presentatie beter kan.	<input type="checkbox"/>	X	<input type="checkbox"/>	<input type="checkbox"/>	<input type="checkbox"/>
7. De conclusie / het eindresultaat is helder en sluit aan bij de onderzoeksraag / ontwerpdoel.	X	<input type="checkbox"/>	<input type="checkbox"/>	<input type="checkbox"/>	<input type="checkbox"/>
8. Alleen voor de eindpresentatie invullen als je ook de tussenpresentatie hebt beoordeeld: De eindpresentatie is beter dan de tussenpresentatie.	<input type="checkbox"/>				
9. De hoeveelheid materiaal is logisch voor de gewenste lengte van de presentatie (1 = te kort, 3 is goed, 5 = te lang)	<input type="checkbox"/>	X	<input type="checkbox"/>	<input type="checkbox"/>	<input type="checkbox"/>

Gebruik deze ruimte voor aanvullende opmerkingen over de presentatie.

Duidelijke presentatie, goed gebruik gemaakt van figuren en het verhaal is goed te volgen. Wat ik handig vond was het uitzoomen om te laten zien waar de Haringvliet is, dit zou ik ook toevoegen in het rapport. De figuren waren duidelijk, alleen ontging het me wat de formule die je liet zien precies inhoudt.

STARTNOTITIE

BRP PERFORMANCE OF WAVE BREAKER FORMULATIONS IN SWAN

AUTHOR: Matthijs (M.I.O.) Wanrooij, 5142040

m.i.o.wanrooij@student.tudelft.nl

SUPERVISOR: Dr. ir. M. (Marcel) Zijlema

m.zijlema@tudelft.nl, room 2.92.1.

DURATION: 13-02-2023 – 03-04-2023

Project description

Wave breaking in the surf zone involves dissipation of wave energy. At the same time, the nonlinear near resonant triad wave interaction (which transfers energy from the spectral peak to super harmonics) increases in decreasing water depth. The transformation of waves over the irregular bottom topography of the coastal zone is modelled by various processes based on empirical parametrizations, which are assumed as independent source/sink terms in the governing action balance equation. These terms are to some extent interdependent because their formulation depends on the same integral wave parameters. This project aims to investigate the interaction between the depth-induced wave breaking source term and the nonlinear triad source term in SWAN-model. This is done in two steps:

1. First, the effect of both the breaking and the nonlinear term on the wave spectrum is assessed by means of a comparison between modelled SWAN-spectra and measured 1D-spectra around the shoal *Hinderplaat* during a storm;
2. Secondly, to assess the isolated impact of the nonlinear triad source term on surf breaking, the dissipation coefficient proposed by Mase and Kirby (1992) is determined by means of both measured spectra and modelled SWAN-spectra without taking the depth-induced wave breaking source term into account.

Research Question

How do the depth-induced wave breaking source term and the nonlinear triad source term interact in wave breaking spectra simulated by the SWAN-model?

Knowledge gaps and suggested literature

The paper that features most of the relevant concepts and formulas for this project is (Saprykina et al., 2022). The paper is highly technical in nature and a thorough understanding of its contents may require further reading on the following topics:

- spilling/plunging type
- What are the relevant wave parameters?
- Phase resolving vs. phase averaged wave models
- LTA (lumped triad approximation) vs. SPB (stochastic parametric model)
- biphase
- breaking index
- Boussinesq equations
- Wave action balance equation (eq. 6)
- *The ‘nonlinear transformation’*
- Local bispectrum
- Self-self interactions
- Ursell number

Bibliography

- [1] J. Battjes and Hans Janssen. “Energy loss and set-up due to breaking random waves”. In: *Proceedings of the 16th International Conference on Coastal Engineering* 1 (Aug. 1978). DOI: 10.9753/icce.v16.
- [2] Y. Eldeberky. “Parameterization of triad interaction in wave energy model”. In: *Proc. Coastal Dynamics Conf. Gdansk, Poland, 1995* (1995). URL: <https://cir.nii.ac.jp/crid/1573387450383923968>.
- [3] Hajime Mase and James T. Kirby. “Hybrid Frequency-Domain KdV Equation for Random Wave Transformation”. In: *Coastal Engineering 1992*. 1992, pp. 474–487. DOI: 10.1061/9780872629332.035. eprint: <https://ascelibrary.org/doi/pdf/10.1061/9780872629332.035>. URL: <https://ascelibrary.org/doi/abs/10.1061/9780872629332.035>.
- [4] James Salmon and Leo Holthuijsen. “Modeling depth-induced wave breaking over complex coastal bathymetries”. In: *Coastal Engineering* 105 (Nov. 2015), pp. 21–35. DOI: 10.1016/j.coastaleng.2015.08.002.
- [5] Yana Saprykina, Burak Aydoğan, and Berna Ayat. “Wave Energy Dissipation of Spilling and Plunging Breaking Waves in Spectral Models”. In: *Journal of Marine Science and Engineering* 10 (Feb. 2022), p. 200. DOI: 10.3390/jmse10020200.

Desired (final) product

The final project will be a report that contains a summary, the problem description, a brief overview of advances and current challenges in the field, a section elaborating on the analysis procedure in SWAN, a critical discussion of results and a conclusion. In addition, the report will feature a preface and bibliography, and optionally a nomenclature and an appendix with source code. For the structure of the final report, please refer to the section ‘Structure of the final report’ at the end of this document.

The main body of the report should be around 20 pages A4.

Plan van aanpak (PVA)

The project aims to determine the interaction between the depth-induced wave breaking source term and the nonlinear triad source term in SWAN. To quantify this interaction, a Python script will be developed to numerically approximate the dissipation coefficient as featured in eq. (1) from (Saprykina et al., 2022). There are two important questions to answer:

- Which breaker formulations will be used?
- Which tests will be performed within the framework of these formulations to assess the interaction?

The approach is outlined in the methods section in the Overleaf document, for which I have provided the link below.

Planning

DATE	TIME	(PLANNED) ACTIVITIES	WEEKLY PLANNING
13-02-2023			
14			Read (Saprykina, 2022) Install SWAN
15			Do SWAN introductory exercises
16			Work on startnotitie
17			Overleaf setup
18			
19			
20			
21		10:00 kick-off meeting kamer 2.92.1 I worked on thinking off a Python routine to process SWAN output files. I first tried using oceanwaves package, but it became clear that this package is deprecated and relies on old versions of various other packages. I then tried to install wavespectra package. Ran into a lot of problems because of dependencies.	Kick-off meeting Discuss starnotitie & make amends Hand in startnotite Read suggested literature Work on introduction
22		Today I continued work on creating a Python routine. Due to the complications of properly installing the wavespectra package, in the process I cluttered and damaged my conda root environment such that today the only option I saw was to completely clean up my system, reinstall conda and start from scratch this time using environments to avoid dependency conflicts. After finally having installed wavespectra successfully in a separate environment, I spent the rest of the afternoon trying to make it interpret NetCDF files, because the output format of the swn command file was .nc. Contacted Prof. Zijlema who informed me that output format is plain text (txt) because outputting in .nc isn't an	

		<p>option in the Windows version of SWAN. Meanwhile I had also asked for help and we managed to confirm the .nc files generated by SWAN were not really NetCDF format because ncdump and nccopy (part of netcdf utilities run on a Linux system) gave the output:</p> <pre>ncdump westh.nc ncdump: westh.nc: NetCDF: Unknown file format</pre> <p>Knowing this, I used another function from the wavespectra package to interpret the SWAN output as SWAN ASCII file and this worked, but only for SPEC2D files (doesn't handle SPEC1D files). For SPEC1D files, I wrote a Python script myself which can extract the data and plot such things as VaDens vs. frequency. This script has some limitations and is not very flexible. It needs manual input detailing the number of locations and the number of frequencies, and assumes the header size remains constant (same number of rows for each file). I hope this is enough flexibility for this project, otherwise I will need to come up with a more sophisticated system to extract data from SPEC1D files.</p>	
23			
24		Inleveren startnotitie (projectomschrijving, pva, planning, structuur rapport)	
25		Build spectrum analyzer	
26		Build spectrum analyzer	
27		Build spectrum analyzer Work on introduction	Read suggested literature Finish introduction
28		Build spectrum analyzer Work on introduction	Work on section Discussion of results Compose tussenrapport
01-03-2023		Build spectrum analyzer Work on introduction	Start on Python implementation Discuss tussenrapport & make amends
02		10:00 meeting prof. Zijlema kamer 2.92.1 Work on introduction	
03		SWAN-simulation, adapt spectrum analyzer Work on methods section	
04		SWAN-simulation, adapt spectrum analyzer Work on methods section	
05		SWAN-simulation, adapt spectrum analyzer Work on methods section	
06		Work on methods section	Python implementation
07		Finish tussenrapport	Start on section Discussion of results

08		Inleveren tussenrapport Prepare presentation + peer feedback	Tussenrapport, final touch
09		Prepare presentation + peer feedback	
10		Tussenrapport presentaties en mondelinge feedback	
11		-	
12		-	
13		Run final simulations Make and tune figures	Python implementation, final touch Complete section Discussion of results
14		Run final simulations Make and tune figures	
15		Run final simulations Make and tune figures	
16		Work on discussion of results Make and tune figures	
17		Work on discussion of results Make and tune figures	
18		-	Python implementation, extra time Conclusion + summary + preface
19		-	
20		14:00 meeting prof. Zijlema kamer 2.92.1 Work on discussion of results Make and tune figures	
21		Work on discussion of results Make and tune figures	
22		Conclusion	
23		General work on the report (expand/correct/layout etc.)	Python implementation, extra time Report, final touch
24		General work on the report (expand/correct/layout etc.)	
25		Work on statistical testing	
26		Work on statistical testing	
27		General work on the report (expand/correct/layout etc.)	
28		General work on the report (expand/correct/layout etc.)	
29		General work on the report (expand/correct/layout etc.)	
30		General work on the report (expand/correct/layout etc.)	
31		Read Chen et al. (1997) and Kuznetsov and Sparykina (2004) and discuss/compare results	
01-04-2023		Final touches	
02		Final touches	
03		Deadline eindrapport	

04			
05		Eindpresentatie	

Structure of the final report

<https://www.overleaf.com/read/mqqzyrrgycjw>